



ELSEVIER

Contents lists available at [ScienceDirect](http://ScienceDirect)

## Journal of Membrane Science

journal homepage: [www.elsevier.com/locate/memsci](http://www.elsevier.com/locate/memsci)

## Highly ionic-conductive crosslinked cardo poly(arylene ether sulfone)s as anion exchange membranes for alkaline fuel cells



Yi Zhi Zhuo, Ao Nan Lai, Qiu Gen Zhang\*, Ai Mei Zhu, Mei Ling Ye, Qing Lin Liu\*

Fujian Provincial Key Laboratory of Theoretical and Computational Chemistry, Department of Chemical &amp; Biochemical Engineering, The College of Chemistry and Chemical Engineering, Xiamen University, Xiamen 361005, PR China

## ARTICLE INFO

## Article history:

Received 20 March 2015

Received in revised form

12 May 2015

Accepted 16 May 2015

Available online 6 June 2015

## Keywords:

Cardo poly(arylene ether sulfone)s

Anion exchange membranes

Fuel cells

Crosslinking

Quaternization

## ABSTRACT

Anion exchange membrane fuel cells (AEMFCs) have become one of the most promising energy-conversion devices due to the potential of adopting non-noble metal catalysts and faster oxygen reduction reaction kinetics in an alkaline operating environment. Here, a series of anion exchange membranes with high ionic-conductivity and low swelling ratio were prepared from imidazolium-functionalized crosslinked cardo poly(arylene ether sulfone)s for AEMFCs. Two oligomers, tertiary amine-containing poly(arylene ether sulfone) (PES-DA) and bromomethyl-containing poly(arylene ether sulfone) (BPES), are synthesized and then mixed at  $-40\text{ }^{\circ}\text{C}$ . They are spontaneously inter-crosslinked at room temperature to form dense anion exchange membranes (AEMs), in which the tertiary amine groups of PES-DA rapidly react with the bromomethyl groups of BPES to form the crosslinked bonds. This avoids the use of crosslinking agents and the expense of functional groups. The resulting membranes show a high hydroxide conductivity up to  $82.4\text{ mS cm}^{-1}$  at  $80\text{ }^{\circ}\text{C}$  and a slight swelling low to traditional AEMs due to its crosslinked network structure. An open circuit voltage (OCV) of  $0.82\text{ V}$  and a maximum power density of  $92.1\text{ mW cm}^{-2}$  are achieved in a  $\text{H}_2/\text{O}_2$  single cell. The as-prepared membranes have a great potential for the application in AEMFCs.

© 2015 Elsevier B.V. All rights reserved.

## 1. Introduction

Proton exchange membrane fuel cells (PEMFCs) have become one of the most promising energy-conversion devices due to their high power density, high energy conversion efficiency, environmental friendliness and ease of fuel supplement [1,2]. Proton exchange membranes (PEMs), the key components for PEMFCs, have been extensively studied. Of those PEMs, Nafion<sup>®</sup> (DuPont), with high proton conductivity and an excellent stability, is the most promising and state-of-the-art polymer electrolyte membranes for PEMFCs. Unfortunately, it also has high fuel permeability. Besides, the high cost membranes and low durability of catalysts also hamper PEMFCs' commercialization [3–5]. Thus, anion exchange membrane fuel cells (AEMFCs) have drawn much more attention for their significant advantages, such as potential of adopting non-noble metal catalysts, faster oxygen reduction reaction kinetics, and lower cost membrane materials than proton exchange membrane fuel cells [6].

Anion exchange membranes (AEMs), one of the key components for AEMFCs, act as hydroxide ion transporter and fuel/oxidant barrier simultaneously. Compared with PEMs,

conductivity is the first important issue to be improved greatly [7]. Therefore, great efforts have been made to enhance the hydroxide conductivity [8]. However, because the conductivity of  $\text{OH}^-$  is much lower than that of  $\text{H}^+$  in an aqueous phase, a higher density of conductive groups is required in AEMs to obtain a high conductivity [9]. Paradoxically, a high density of conductive groups will lead to a poor dimensional stability, mechanical stability and solvent resistance of AEMs [10]. This makes it impossible to construct membrane electrode assembly (MEA). An effective and direct approach to solve this problem is to crosslink the polymer chain [11,12]. In most cases, crosslinking was conducted by introducing a micromolecular crosslinker to combine neighboring polymers or bonding halomethyl groups ( $-\text{CH}_2\text{Cl}$  or  $-\text{CH}_2\text{Br}$ ) with aromatic rings of near polymer chains [10–16]. The first pathway mentioned above needs to introduce a separate crosslinker molecule. However, if the adscititious crosslinker has a distinctive molecular structure that is incompatible with the polymer chain, some problems may emerge. This will lead to a poor membrane quality or even make crosslinking unsuccessful [16]. The second approach requires the expense of halomethyl groups, which can be converted to quaternized ammonium, imidazolium or guanidinium, thus it will inevitably cause a significant reduction in conductivity. Recently, Lu et al. [17] and Rao et al. [18] reported an approach to crosslink the polymer through quaternization or

\* Corresponding authors. Tel.: +86 592 2188072; fax: +86 592 2184822.

E-mail addresses: [qgzhang@xmu.edu.cn](mailto:qgzhang@xmu.edu.cn) (Q.G. Zhang), [qlliu@xmu.edu.cn](mailto:qlliu@xmu.edu.cn) (Q.L. Liu).

imidazolium reaction. Compared with the two mentioned above, this way avoids the utilization of a micromolecular crosslinker and expense of functional groups.

Poly(arylene ether sulfone) (PES) is a kind of thermoplastic polymers with good mechanical property, excellent thermal stability and anti-corrosion performance, so numerous polymers based on PES were synthesized from monomers or by polymer modifications and show promising for AEMFCs [4,14–16]. In our previous works, we have successfully designed and synthesized a series of novel quaternized fluorene-containing PES for AEMs [19,20]. The monomer tetramethyl bisphenol fluorene provides four functional points, thus the number of ionic groups in each polymer repeating unit can be increased. However, the swelling ratio of the as-prepared AEMs may be too high to be used in practice by increasing ionic groups.

Herein, a series of imidazolium crosslinked polymers were prepared for AEMFCs (Fig. 1). We have synthesized cardo poly(aryl ether sulfone) containing pendent tertiary amine groups (PES-DA) and brominated poly(aryl ether sulfone) containing tetramethyl bisphenol fluorene (BPES). Both of the polymers contain cardo-type molecules, phenolphthalein or fluorene groups, which could force each polymer chain apart leading to large interchain separations (free volume) in which water molecules could be confined [21,22]. PES-DA solution and BPES solution are mixed at  $-40\text{ }^{\circ}\text{C}$ , followed by the fabrication of membranes at room temperature (RT), and a crosslinking reaction is taking place during the membrane formation. The formed crosslinkage is quaternary ammonium group, which can also serve as hydroxide conductors. The membranes were then soaked in a 1-methylimidazole solution to convert the remaining bromomethyl groups into imidazolium groups. All of these result in imidazolium crosslinked AEMs with high ionic conductivity and suppressed swelling ratio. An open circuit voltage (OCV) of 0.82 V and a maximum power density of  $92.1\text{ mW cm}^{-2}$  at a current density of  $244\text{ mA cm}^{-2}$  can be achieved in a single cell evaluation.

## 2. Experimental

### 2.1. Materials

Silicotungstic acid (AR), 1-methylimidazole (MIM, 99%), 2,6-dimethylphenol (99%) and 9-fluorenone (99%) were purchased from Aladdin Industrial Inc. Phenolphthalein (PPH, 98%) and bis(4-fluorophenyl) sulfone (FPS, 99.0%) were obtained from TCI (Shanghai) Development Co., Ltd. N,N-dimethylethane-1,2-diamine (DMDA, 99%) was supplied from J&K Scientific Ltd. Toluene and N,N-dimethylacetamide were stirred over CaH<sub>2</sub> for 24 h, then distilled under reduced pressure and stored over 4 Å molecular sieves. Benzoyl peroxide (BPO) was recrystallized from chloroform. All other chemicals were supplied from Shanghai Sinopharm Chemical Reagent Co., Ltd (China) and used without further purification.

### 2.2. Preparation of AEMs

The diagram for preparation of the AEMs is shown in Scheme 1. The monomers 2-(2-(dimethylamino)ethyl)-3,3'-bis(4-hydroxyphenyl)isoindolin-1-one (PPH-DA) and 9,9'-bis(4-hydroxy-3,5-dimethylphenyl) fluorene (DMBHF) were synthesized from the raw materials. Tertiary amine-containing poly(arylene ether sulfone) (PES-DA) and benzylmethyl-containing poly(arylene ether sulfone) (MPES) were prepared via nucleophilic substitution copolymerization. Bromomethyl-containing poly(arylene ether sulfone) (BPES) was made from MPES. PES-DA solution and BPES solution were first mixed at  $-40\text{ }^{\circ}\text{C}$ , and the mixture was then used to prepare membranes at RT. The as-prepared membranes were further treated by a 1-methylimidazole solution, making the remaining  $-\text{CH}_2\text{Br}$  groups be converted into imidazolium groups.

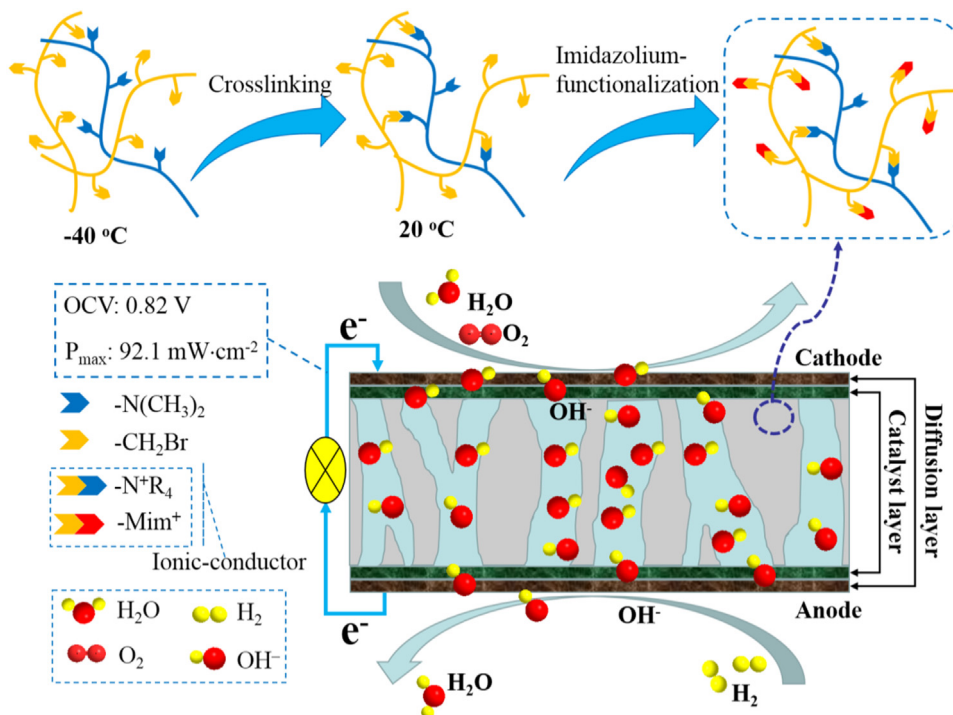
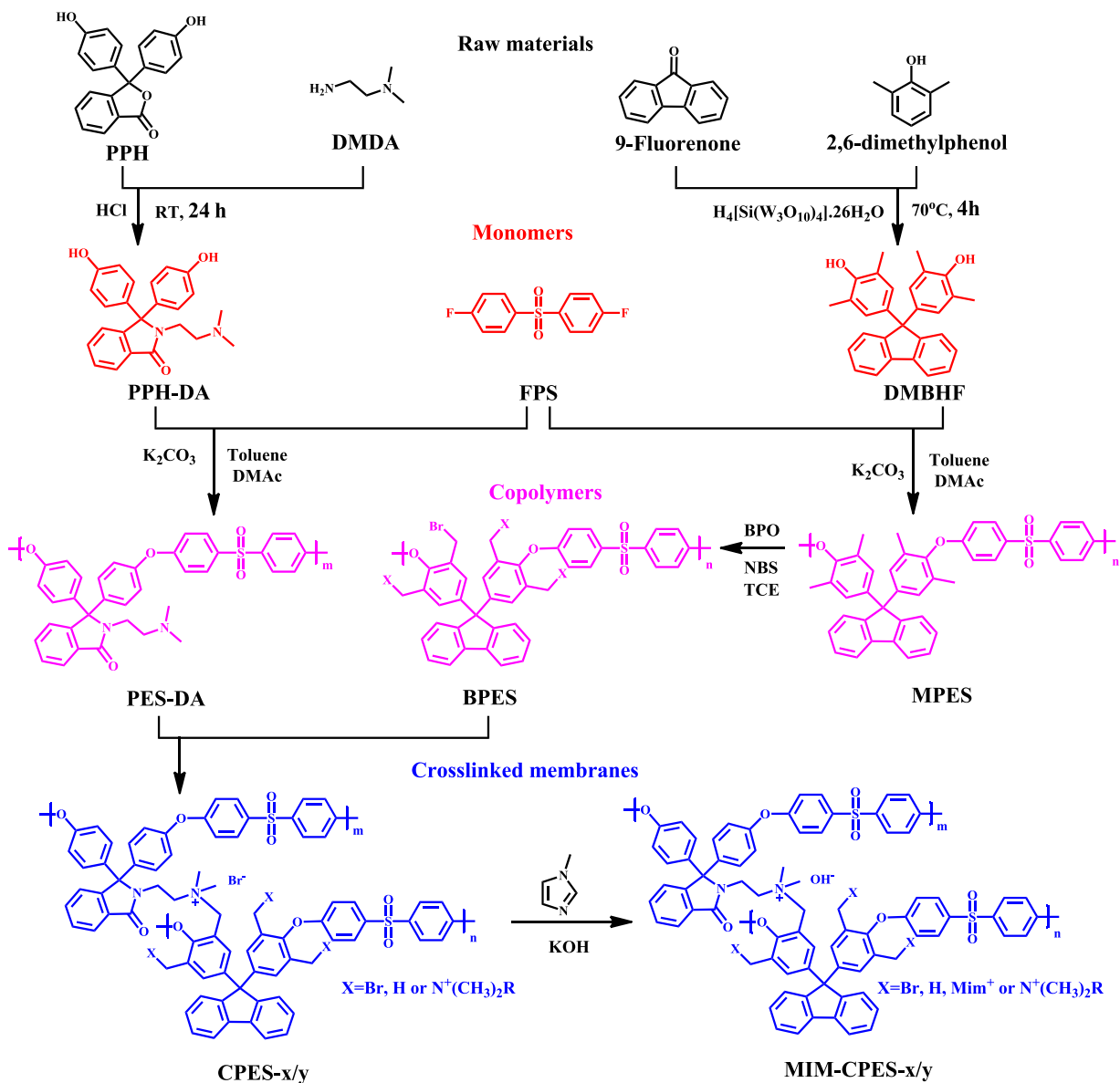


Fig. 1. Fabrication of the crosslinked membrane and single cell testing.



**Scheme 1.** Reactions for the synthesis of crosslinked AEMs.

### 2.2.1. Monomers synthesis

PPH-DA was synthesized by the method described in the literature [23], as shown in Scheme 1. PPH (19.0992 g, 60 mmol), concentrated hydrochloric acid (5 mL) and DMDA (36 mL) were added into a 100 mL three-necked flask equipped with a mechanical stirrer, a condenser, a nitrogen inlet and outlet. The mixture was refluxed at RT for 24 h. Afterwards, the solution was poured into deionized (DI) water to give a precipitate, followed by filtration and washing with DI water for several times. The crude product was then recrystallized from a mixture of ethanol and water to obtain a pure crystal product (yield: 75%).

The DMBHF was prepared according to the method reported in the literature [19]. A 250 mL three-necked flask equipped with a magnetic stirrer, a condenser and a thermometer was charged with 9-fluorenone (18.20 g, 0.10 mol), excess of 2,6-dimethylphenol (61.08 g, 0.50 mol) and silicotungstic acid (1.2 g). The mixture was stirred at 70 °C for 4 h under a reduced pressure of  $1.3 \times 10^3$  Pa, then 1.2 g of a 29 wt% NaOH solution was added to cease the reaction. 125 g of toluene and 35 g of DI water were added into the above mixture under vigorous stirring to give a phase separation. After removing the aqueous phase, the organic

phase was washed twice with DI water and cooled to 10 °C leading to crystallization. After filtration, the residue was washed with DI water to yield a crude product. The crude product was then recrystallized from toluene twice to obtain a pure white powder of DMBHF (yield: 78%).

### 2.2.2. Synthesis of PES-DA and MPES

The synthesis of PES-DA and MPES via nucleophilic substitution copolymerization is shown in Scheme 1. A typical procedure for the synthesis of PES-DA is described as follows. A 100 mL three-necked flask equipped with a magnetic stirrer, a condenser and a thermometer was charged with PPH-DA (1.9423 g, 5 mmol) (where the monomer DMBHF was used for the synthesis of MPES), FPS (1.2713 g, 5 mmol), K<sub>2</sub>CO<sub>3</sub> (1.38 g, 10 mmol), toluene (8 mL) and DMAc (15 mL). The reaction mixture was heated to 140 °C under nitrogen for 4 h. Meanwhile, dehydration was proceeded by removing the azeotrope formed from the toluene and water out of the reaction system. The temperature was raised slowly to 165 °C and then the reaction was continued for another 20 h. The viscous solution was cooled to RT and then diluted with DMAc. Afterwards, the mixture was poured into

400 mL of an aqueous methanol solution under stirring (methanol/deionized water=1/1, v/v) to produce a yellowish solid precipitate (while MPES is a white solid precipitate). The precipitate was magnetically stirred at 80 °C for another 4 h, collected by filtration, Soxhlet extracted with methanol overnight and dried at 80 °C under vacuum for 24 h to yield a yellowish solid product (while MPES is a white solid product). The chemical structure of the as-synthesized copolymer was characterized using  $^1\text{H}$  NMR and FT-IR.

### 2.2.3. Bromination of MPES

The radical substitution bromination reaction of the benzylmethyl-bearing poly(sulfone)s was carried out in 1,1,2,2-tetrachloroethane (TCE), using N-bromosuccinimide (NBS) as the bromination agent and benzoyl peroxide (BPO) as the initiator (Scheme 1) [19]. A 100 mL three-necked round-bottomed flask equipped with a condenser, a magnetic stirrer, and a gas inlet and outlet was charged with MPES (3.0000 g) and TCE (60 mL). The mixture was heated to 85 °C in a nitrogen atmosphere. After the MPES being dissolved completely, 3.7880 g of NBS and 0.5155 g of BPO were added. The mixture was stirred at 85 °C under the protection of nitrogen for 5 h. The solution was then cooled to RT, and poured into 400 mL of methanol under stirring followed by filtration to yield a crude solid. The crude product was washed with methanol for several times and vacuum dried at 60 °C for 24 h to obtain a yellow solid. The product is termed BPES, where B denotes the bromination reaction. The chemical structure of the BPES was characterized using  $^1\text{H}$  NMR and FT-IR.

### 2.2.4. Fabrication of the crosslinked membranes (CPES- $x/y$ ) and the imidazolium crosslinked membrane (MIM-CPES- $x/y$ )

The reactions for preparation of the crosslinked AEMs are shown in Scheme 1. Fig. 2 also presents the procedure for synthesis of the crosslinked membranes in detail. PES-DA and BPES were completely

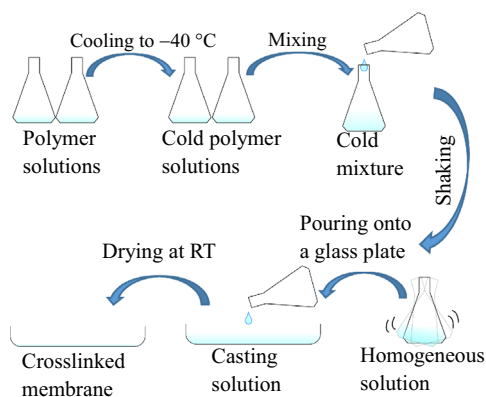


Fig. 2. Fabrication of the crosslinked membranes (CPES- $x/y$ ).

dissolved in  $\text{CHCl}_3$  separately (3% w/v), the solutions were filtered through a 0.45  $\mu\text{m}$  filter and cooled to  $-40$  °C. Both the cold BPES ( $x$  mL) and PES-DA ( $y$  mL) solutions were then mixed. The resulting mixture was vigorously shaken to obtain a homogeneous solution. The solution was then poured onto a glass plate, and dried at RT for 12 h to form a membrane. The as-prepared membrane is termed CPES- $x/y$ , where  $x/y$  is the volume ratio of BPES to PES-DA. Herein, three membranes CPES-2/2, CPES-2.5/1.5 and CPES-3/1 were prepared. Subsequently, the CPES- $x/y$  membrane was immersed in a solution of 1-methylimidazole diluted by ethanol (v/v, 1/2) at 30 °C for 96 h. After that, the membrane was further submerged in a 1 M aqueous KOH solution for 48 h, converting the membranes from the  $\text{Br}^-$  form into the  $\text{OH}^-$  form. After alkalization, the membranes were put into DI water for more than 24 h before use. The resulting membranes are termed MIM-CPES- $x/y$ , where MIM denotes the imidazolium reaction.

### 2.2.5. Structure characterization

$^1\text{H}$  NMR spectra were recorded by Avancell 500 MHz (Bruker, Switzerland) using  $\text{CDCl}_3$  or  $\text{DMSO-d}_6$  as the solvent and tetramethylsilane (TMS) as the internal reference. FT-IR spectra were recorded in the range 4000–500  $\text{cm}^{-1}$  on the membrane samples using a Nicolet Avatar 380 spectrophotometer (Thermo Electron Corporation, USA). The molecular weights of the polymers were measured using a GPC (Waters, USA) equipped with a Waters 1515 isocratic HPLC pump, three Styragel columns (Waters HT4, HT5E and HT6) and a Waters 2414 refractive index detector. Molecular weight was determined at 30 °C using polystyrene samples as the standard. The morphology and microstructure of the membranes were characterized using a field emission scanning electron microscope (SEM, Zeiss Sigma, Germany). The elemental analysis of the membranes was carried out on the SEM equipped with an EDX detector (Oxford Inca). All of the samples were fractured in liquid nitrogen and then sputtered with gold before observation. Thermal stability of the membranes was evaluated using a thermogravimetric analyzer (SDT-Q600, TA, USA) from 30 to 800 °C at a heating rate of 10 °C  $\text{min}^{-1}$  under a nitrogen atmosphere. The membranes were dried at 60 °C under vacuum for 48 h before testing. X-ray photoelectron spectroscopy (XPS) was recorded on a PHI QUANTUM 2000 XPS system with Al  $K\alpha$  source. All the binding energies were referenced to the C 1S peak at 284.8 eV of the surface adventitious carbon. The mechanical

Table 1  
Molecular weight, polydispersity index (PDI) of MPES and PES-DA.

Copolymers	Mw ( $10^3$ Da)	Mn ( $10^3$ Da)	PDI
MPES	14.07	9.00	1.56
PES-DA	6.34	4.94	1.28

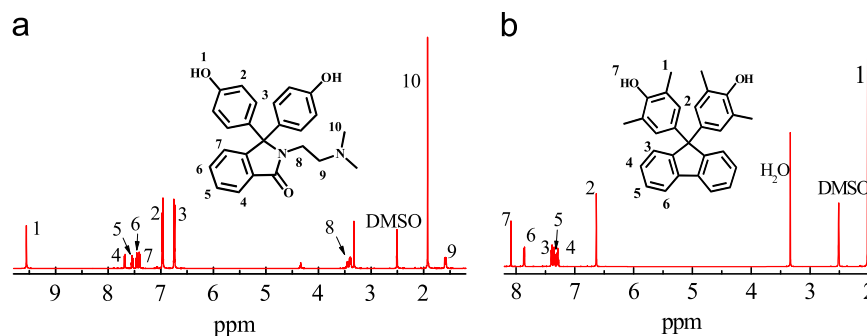


Fig. 3.  $^1\text{H}$  NMR spectra of (a) PPH-DA and (b) DMBHF.

properties of the AEMs were measured using a universal testing machine (WDW-1E Testing System) with an elongation speed of 5 mm min<sup>-1</sup> at RT. A 10 mm wide membrane was kept in DI water at RT overnight and was taken out to remove the surface water using a tissue before the measurements.

### 2.3. Characterizations of MIM-CPES-x/y membranes

#### 2.3.1. Ionic conductivity

The resistance of the membrane samples was measured by the two-electrode AC impedance spectroscopy method on a Parstat 263 electrochemical workstation (Princeton Advanced Technology, USA). The test was performed at a constant voltage of 10.0 mV in the frequency range from 100 mHz to 100 kHz. Before testing, the OH<sup>-</sup> form membranes were hydrated in DI water for at least 48 h. The testing device with a 1 × 3 cm<sup>2</sup> membrane was clamped between two copper electrodes and then placed in a N<sub>2</sub>-protected chamber with DI water to maintain a relative humidity (RH) of 100% during the measurements. The ionic conductivity,  $\sigma$  (S cm<sup>-1</sup>), is calculated as follows:

$$\sigma = \frac{l}{AR} \quad (1)$$

where  $l$  (cm) is the distance between the two electrodes,  $A$  (cm<sup>2</sup>) is the cross-sectional area of the tested membrane and  $R$  is the membrane resistance from the AC impedance data ( $\Omega$ ).

#### 2.3.2. Water uptake (WU)

The WU was examined using a quartz spring balance after the membranes were vacuum dried at 60 °C for 48 h by the method reported in the literature [20]. The WU of the membrane can be calculated by Hooke's law

$$WU = \frac{kL_3 - kL_2}{kL_2 - kL_1} \times 100\% = \frac{L_3 - L_2}{L_2 - L_1} \times 100\% \quad (2)$$

where  $k$  is the elasticity coefficient of the quartz spring,  $L_1$  is the original length of the quartz spring,  $L_2$  is the length of the quartz spring loaded with a dried membrane, and  $L_3$  is the length of the quartz spring loaded with the swollen membrane.

#### 2.3.3. Swelling ratio (SR)

The SR of the membrane was measured in the plane direction and is calculated by

$$SR = \frac{(L_w \times W_w)^{1/2} - (L_d \times W_d)^{1/2}}{(L_d \times W_d)^{1/2}} \times 100\% \quad (3)$$

where  $L_w$  and  $W_w$  are the length and the width of the wet membranes, respectively, and  $L_d$  and  $W_d$  are the length and the width of the dried membranes, respectively.

#### 2.3.4. Ionic exchange capacity (IEC)

The classical back titration method was used to determine the IEC of the AEMs. The OH<sup>-</sup> form membrane was immersed into 30 mL of a 0.01 M HCl solution for 24 h to ensure that all OH<sup>-</sup> was fully exchanged by Cl<sup>-</sup>. The solution and the membrane were then back titrated with a 0.01 M KOH solution. The IEC (meq g<sup>-1</sup>) is calculated by

$$IEC = \frac{M_{o, HCl} - M_{e, HCl}}{m_d} \times 100\% \quad (4)$$

where  $M_{o, HCl}$  and  $M_{e, HCl}$  (mol L<sup>-1</sup>) are the milliequivalents (meq) of HCl required before and after equilibrium, respectively, and  $m_d$  is the mass of the dried membranes (g).

#### 2.3.5. Alkaline stability

The alkaline stability of AEM was investigated by monitoring the variation of conductivity after the membrane was immersed in a 2 M KOH solution at 60 °C for different time from 24 to 502 h. The AEMs were then placed into DI water for more than 24 h before testing.

### 2.4. Membrane electrode assembly (MEA) and single cell performance

The anode and cathode catalysts were prepared as follow: Pt/C (40 wt% Pt, Johnson Matthey) and homemade ionomer was mixed with a weight ratio of 6/4 in DMSO and glycerol. The resulting mixture was ultrasonically dispersed for 15 min and then vigorously stirred for 24 h to make a homogenous dispersion.

The catalyst ink was sprayed on a Teflon-treated carbon paper (Toray-250). The Pt loading for both the electrodes was 1 mg cm<sup>-2</sup>. The MEAs with an active area of 2 × 2 cm<sup>2</sup> were fabricated by hot-pressing the anode and cathode electrodes on

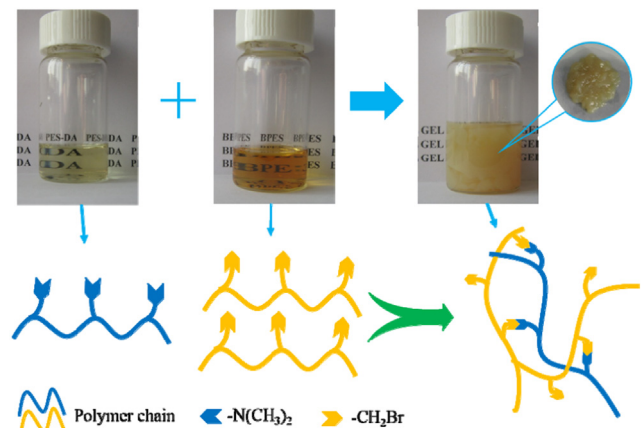


Fig. 5. The schematic of gel formation at room temperature (RT).

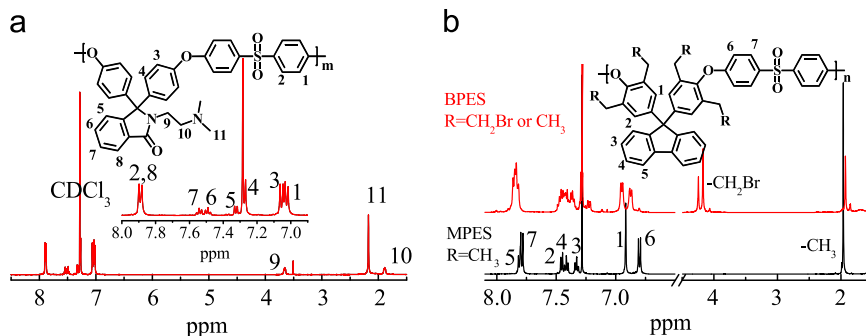


Fig. 4. <sup>1</sup>H NMR spectra of (a) PES-DA, (b) MPES and BPES.

both sides of the MIM-CPES-3/1 membrane at 50 °C for 10 min. The MEA was then immersed in DI water for 24 h and assembled in a single cell for testing.

H<sub>2</sub> on the anode and O<sub>2</sub> on the cathode were fed with a flow rate of 50 and 100 mL min<sup>-1</sup>, respectively. Single cell performance was evaluated at 50 °C with a RH of 100% using an electronic load (ZY8714, ZHONGYING Electronic Co., Ltd.).

### 3. Results and discussion

#### 3.1. Preparation and structure of the MIM-CPES-x/y membranes

##### 3.1.1. Synthesis and characterization of monomers

A typical route for the synthesis of the biphenol monomers (PPH-DA and DMBHF) is shown in Scheme 1. The monomer PPH-DA was synthesized by the method described in the literature [22]. N,N-dimethylethane-1,2-diamine (DMEA) reacted with phenolphthalein in a three-necked flask at RT to produce PPH-DA (yield: 75%). The structure was confirmed by <sup>1</sup>H NMR in DMSO-d<sub>6</sub>. As shown in Fig. 3a, the -OH signal appears at 9.56 ppm, and the signals at 1.93, 3.40 and 1.59 ppm are attributed to the pendant aliphatic chain. 9-Fluorenone reacted with 2,6-dimethylphenol to produce the monomer DMBHF, as reported by our group [19]. This reaction was catalyzed by silicotungstic acid under reduced pressure at 70 °C. The structure of DMBHF was confirmed by <sup>1</sup>H NMR in DMSO-d<sub>6</sub>, as shown in Fig. 3b.

##### 3.1.2. Synthesis and characterization of PES-DA, MPES and BPES

Pendent tertiaryamine-containing PES and benzylmethyl-containing PES were synthesized from PPH-DA and DMBHF, respectively. Table 1 shows the information of the molecular weight of copolymers. Fig. 4a shows the <sup>1</sup>H NMR spectrum of PES-DA, in which all of the aromatic protons are assigned to the proposed polymer structure. The peak at 7.28 ppm is associated with CDCl<sub>3</sub>. The peaks around 2.18, 3.66 and 1.89 ppm are ascribed to the chemical shifts of proton in the pendent chain.

Fig. 4b shows the <sup>1</sup>H NMR spectrum of MPES. All of the aromatic protons are assigned to the proposed polymer structure, and the signal at around 1.96 ppm is assignable to the -CH<sub>3</sub> in DMBHF. The conversion of -CH<sub>3</sub> to reactive -CH<sub>2</sub>Br for grafting was conducted using NBS, BPO and TCE as the brominating agent, initiator and solvent, respectively. As shown in the <sup>1</sup>H NMR spectra of BPES (Fig. 4b), the chemical structure and the degree of bromomethylation of the MPES can be determined. Compared with MPES, new peaks around 4.17–4.24 ppm appeared on the <sup>1</sup>H NMR spectra of BPES are assignable to methylene protons (Fig. 4b). The peak associated with the methyl decreased in size after

bromomethylation. The <sup>1</sup>H NMR spectra suggest the successful bromination on the MPES. The degree of bromomethylation (69.8%) can be yielded by integrating the protons on the bromomethyl groups.

#### 3.1.3. Preparation and characterization of the imidazolium crosslinked PES membranes

The key to prepare the crosslinked membranes is to make a homogenous casting solution. When the PES-DA solution is mixed with the BPES solution (solvent: CHCl<sub>3</sub>, NMP or DMSO) at RT, the mixture tends to be a gel in seconds making the casting of membranes impossible (Fig. 5). The benzyl bromide on the BPES is highly active, and can easily react with the tertiary amine group on the PES-DA, even at RT (Fig. 5). That is the reason for gel formation. Therefore, low temperature was used to control the reactivity in preparing casting solution. The procedure for preparation of the crosslinked AEMs is shown in Scheme 1. Both the PES-DA and BPES solutions were cooled to -40 °C and then mixed under vigorous shaking to obtain a homogeneous solution. The solution was then poured onto a glass plate, and dried at RT. In the casting process, crosslinking reaction would occur resulting in crosslinked membranes. A homogeneous dispersion of the two components is needed for preparation of AEMs. In the compositional mapping images of the CPES-3/1 membrane (Fig. 6a and b), N element on the PES-DA and Br element on the BPES were distributed uniformly in the membrane. This suggests the two polymers forming a homodisperse system.

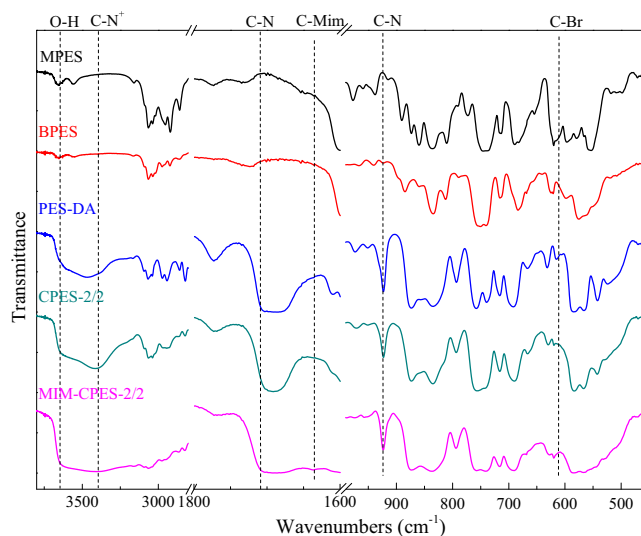


Fig. 7. FT-IR spectra of MPES, BPES, PES-DA, CPES-2/2 and MIM-CPES-2/2.

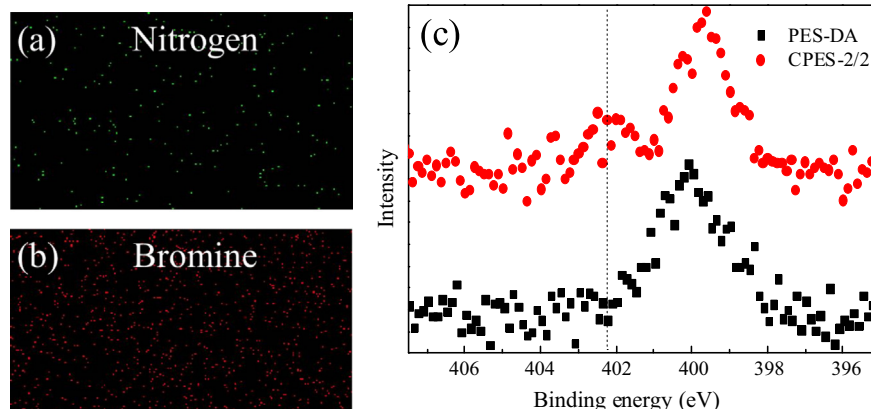


Fig. 6. Compositional mapping images of the CPES-3/1 membrane: (a) N and (b) Br, and (c) XPS spectra of PES-DA and CPES-2/2 membranes.

Furthermore, the change of groups in the preparation of cross-linked membranes was characterized via XPS. The N 1s spectrum of the PES-DA and CPES-2/2 is shown in Fig. 6c. Only one peak (around 400.1 eV) is found in the spectrum of PES-DA, which is attributed to the tertiary amino groups on the PES-DA. A new peak at 402.2 eV appeared in the CPES-2/2 membrane is assignable to quarternary ammonium groups [17].

The CPES-*x/y* membranes were insoluble in commonly used polar organic solvents including CHCl<sub>3</sub>, DMF, DMAc, DMSO, NMP and THF. In the FT-IR spectrum (Fig. 7) of the MPES and PES-DA, the peak at 3376 cm<sup>-1</sup> arises from the stretching vibration of quaternary ammonium salt groups [24]. The band at 602 cm<sup>-1</sup> is ascribed to the stretching vibration of remaining –CH<sub>2</sub>Br groups. All these indicate successful formation of a crosslinked network in the membranes.

Subsequently, the CPES-*x/y* membranes were treated with 1-methylimidazole to convert the unreacted –CH<sub>2</sub>Br groups into imidazolium groups, followed by alkalization with aqueous KOH solution resulting in the MIM-CPES-*x/y* membranes. As shown in Fig. 7, the absorption bands associated with the –CH<sub>2</sub>Br groups disappeared in the FT-IR spectrum of MIM-CPES-*x/y*, while a new peak appeared at around 1634 cm<sup>-1</sup> arising from the vibration of imidazolium cation [25]. Moreover, the EDX spectra revealed that the bromine elements in the CPES-3/1 declined (or almost disappeared) in the MIM-CPES-3/1 membrane (Fig. 8a and b). This evidences the successful introduction of imidazolium into CPES-3/1.

### 3.1.4. Mechanical properties and thermal stability

To undergo the hot-press in the construction of membrane electrode assembly, AEMs must possess sufficient mechanical strength. The mechanical properties of the MIM-CPES-*x/y* membranes are shown in Table 2. The MIM-CPES-*x/y* membranes show tensile strengths between 17.11 and 32.12 MPa and elongation at break varying from 5.97% to 8.45%. The mechanical strength decreased with the IEC values. The tensile strength and elongation at break of the MIM-CPES-3/1 membrane are close to the cross-linked PVAc(3)-c-PVBC(2)/OH [17].

The thermal stability of the crosslinked AEMs was evaluated via TGA (Fig. 9). A slight initial weight loss below ~120 °C is attributed to the evaporation of the water. The second stage, from 240 to 370 °C, is likely due to the decomposition of imidazolium groups. The third weight loss above 380 °C is related to the splitting of the copolymer main chain. In summary, all the cross-linked AEMs exhibit a good thermal stability below 200 °C.

### 3.2. Morphology of the imidazolium crosslinked membranes

The SEM image of the surface and cross-section of the MIM-CPES-3/1 is shown in Fig. 10a and b. The membranes are found to be smooth and compact so that they can be used as the barrier of fuels and the conductor of OH<sup>-</sup>. Furthermore, a uniform and smooth structure with around 40 μm in thickness can be observed. As shown in Fig. 10c, the MIM-CPES-3/1 membrane was transparent, uniform and homogeneous from the photograph. No phase separation was found in it. Fig. 10d shows that the membrane can be curved in any way. This shows that the obtained membranes are flexible enough for fuel cells.

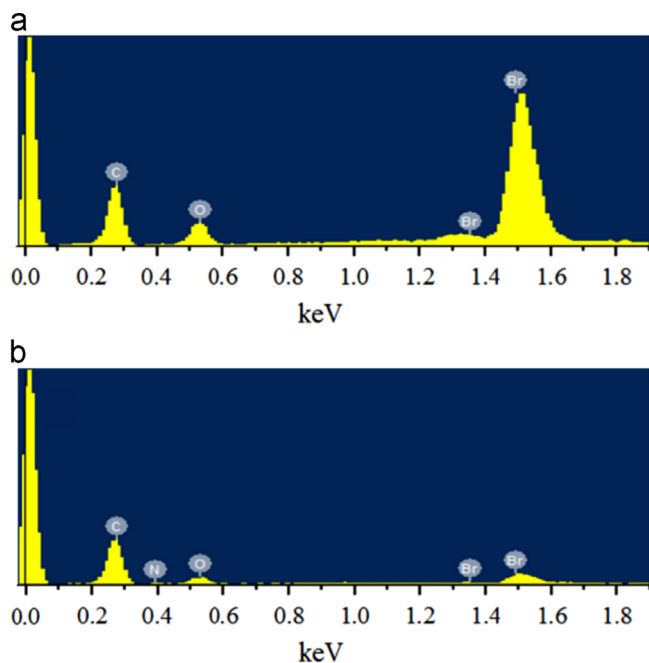


Fig. 8. EDX spectra of the (a) CPES-3/1 and (b) MIM-CPES-3/1 membranes.

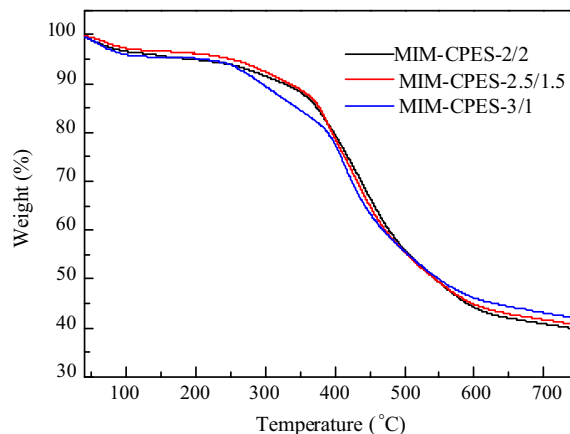


Fig. 9. TGA curves of the AEMs under a nitrogen atmosphere.

**Table 2**  
IEC, water uptake, swelling ratio and mechanical properties of the AEMs.

Membrane	IEC (meq g <sup>-1</sup> )		WU (%)		SR (%)		Tensile strength (MPa)	Elongation at break (%)
	Cal. <sup>a</sup>	Exp. <sup>b</sup>	30 °C	60 °C	30 °C	60 °C		
MIM-CPES-2/2	1.46	0.82 ± 0.03	6.67 ± 0.20	9.04 ± 0.22	2.78 ± 0.10	4.88 ± 0.12	32.12 ± 0.45	8.45 ± 0.18
MIM-CPES-2.5/1.5	1.77	1.13 ± 0.04	7.60 ± 0.21	11.11 ± 0.21	3.84 ± 0.12	6.17 ± 0.12	29.55 ± 0.50	6.02 ± 0.20
MIM-CPES-3/1	2.07	1.37 ± 0.04	8.02 ± 0.19	12.96 ± 0.23	4.60 ± 0.16	7.48 ± 0.15	17.11 ± 0.36	5.97 ± 0.19

<sup>a</sup> Calculated value from the feed ratio.

<sup>b</sup> Experimental value determined by titration.

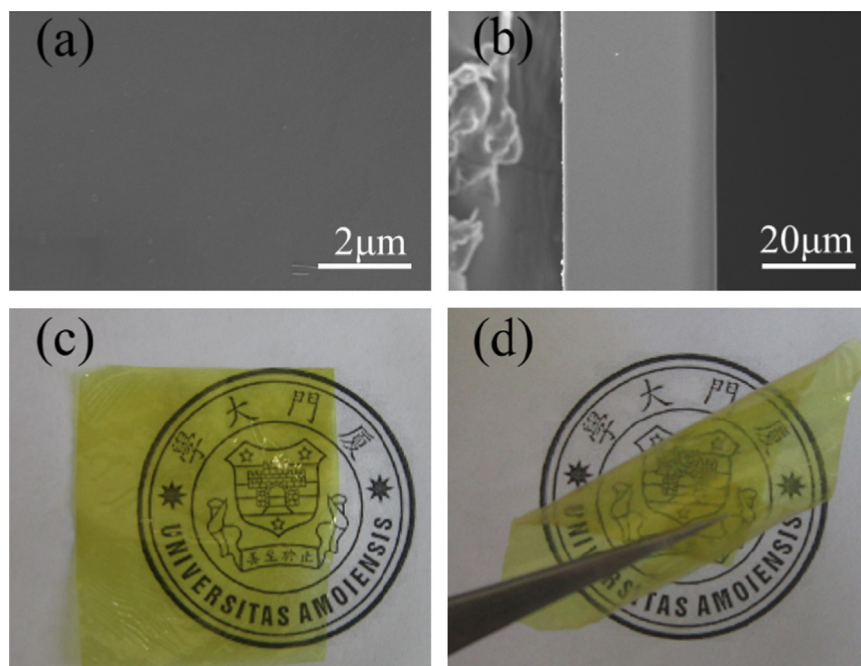


Fig. 10. SEM image: (a) top-view and (b) cross-section, and (c, d) digital photo of the MIM-CPES-3/1 membrane.

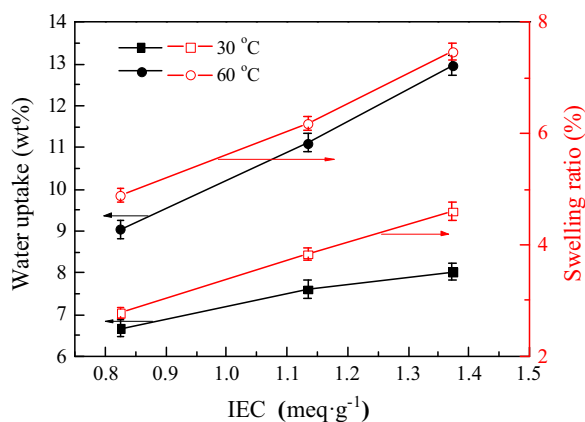


Fig. 11. IEC dependence of water uptake and swelling ratio of the AEMs.

### 3.3. Properties of MIM-CPES-*x/y* membranes

#### 3.3.1. IEC, water uptake (WU) and swelling ratio (SR)

IEC, a basic parameter of an ion exchange membrane, defined as the milliequivalents (meq) of functional groups per gram of the polymer, intimately affects the conductivity and water uptake of membranes. As listed in Table 2, the IEC values of MIM-CPES-*x/y*, determined by titration, increased in the range from 0.82 to 1.37 meq g<sup>-1</sup> with increasing BPES content. A comparison of the theoretic and titrated IEC values shows that the efficiency of the reaction between benzyl bromide groups and 1-methylimidazole in the solid membrane state is around 60%. This is probably due to the large molecular size of 1-methylimidazole which makes it difficult to come into contact with the benzyl bromide groups. Water in the membrane can form a transport channel for hydroxide ions, while excessive water uptake will cause serious swelling and reduce mechanical stability [26].

Both WU and SR of the crosslinked imidazolium membranes are found to increase with increasing IEC and temperature, as shown in Fig. 11. This may be that the imidazolium polymer tends

to be more hydrophilic with increasing IEC. The mobility of both water and polymer chains increased by increasing temperature resulting in a larger free volume [27,28]. As expected, all of the as-prepared AEMs showed much lower swelling than typical AEMs due to the formation of a crosslinked network. The crosslinked network could constrain the motion of water and polymer chains, so even at an elevated temperature, the swelling ratio of the MIM-CPES-*x/y* membranes can also be maintained at a lower level.

#### 3.3.2. Hydroxide conductivity

The hydroxide conductivity of AEMs is critical for fuel cell applications. The ionic conductivity of the MIM-CPES-*x/y* membranes at different temperatures is shown in Fig. 12. The membranes have high conductivity in the range of 19.1–32.2 mS cm<sup>-1</sup> and 47.6–82.4 mS cm<sup>-1</sup> at 30 and 80 °C, respectively. The conductivity increases with increasing temperature due to the faster migration of ions and higher water diffusivity at a higher temperature. All the crosslinked AEMs show a high conductivity at a very low swelling ratio, indicating that these membranes meet the requirement for fuel cells.

To assess the advantage of the as-prepared crosslinked membranes, the ratio of  $\sigma$ /SR is introduced to depict the conductivity against swelling. A membrane with higher  $\sigma$ /SR indicates that a higher conductivity can be obtained at the same swelling ratio. As listed in Table 3, in comparison with the commercial proton exchange membrane Nafion<sup>®</sup> 117 and the currently reported crosslinked AEMs [10,16,28,29], the MIM-CPES-*x/y* membranes are found to have a much higher  $\sigma$ /SR value. The presence of cardo-type structure, phenolphthalein and fluorene groups, could force each polymer chain apart resulting in large interchain separations (free volume) in which water molecules could be confined [21,22]. This will promote the ionic conductivity of AEMs. Furthermore, PES-DA is crosslinked with BPES via quaternization in this work, so that the crosslinkage can also serve as an ion exchange moiety. Therefore, the crosslinked AEMs exhibit a fairly high ionic conductivity.



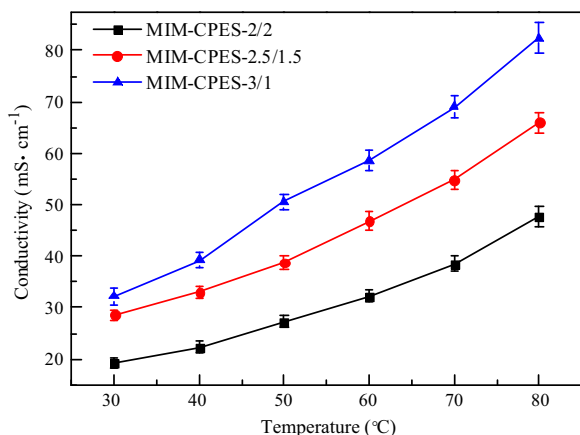


Fig. 12. Temperature dependence of ionic conductivity of the AEMs.

Table 3

Conductivity ( $\sigma$ ), swelling ratio (SR) and  $\sigma$ /SR of the AEMs.

Membrane	Temperature (°C)	$\sigma$ (mS cm <sup>-1</sup> )	SR (%)	$\sigma$ /SR (mS cm <sup>-1</sup> )
MIM-CPES-2/2	30	19.1	2.78	6.89
	60	32.4	4.88	6.60
MIM-CPES-2.5/1.5	30	28.5	3.84	7.44
	60	46.8	6.17	7.59
MIM-CPES-3/1	30	32.2	4.60	6.99
	60	58.6	7.48	7.83
Nafion <sup>®</sup> 117 <sup>a</sup>	30	77.6	19.69	3.94
	60	103.2	25.22	4.09
C-FPAEO-50-MIM [10]	20	6.5	2	3.25
	60	16.9	3	5.63
CPAES-Q-100 [29]	25	22.2	9.6	2.31
	80	42.7	13.7	3.12
100%-1 [28]	30	0.56	0.1	5.6
	60	1.3	0.37	3.51
SCL-TPQPH5.3% [16]	20	38	15	2.53

<sup>a</sup> Measured under the same condition in our laboratory.

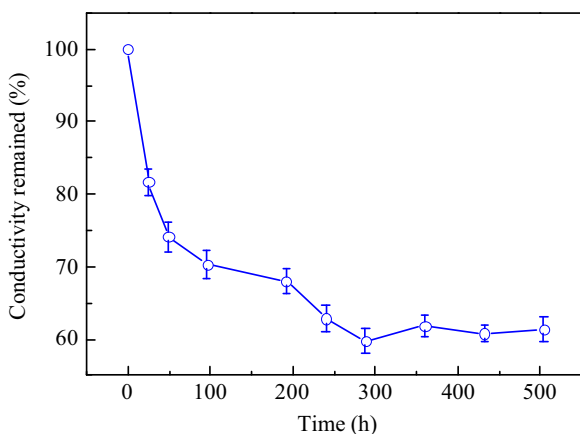


Fig. 13. Alkaline stability of MIM-CPES-3/1 in a 2 M KOH solution at 60 °C.

### 3.3.3. Alkaline stability

The alkaline stability is an important property of AEMs. The AEMs with good alkaline stability will keep a relatively high conductivity under alkaline circumstance for a long time. In this work, the alkaline stability of the MIM-CPES-3/1 membrane was examined by monitoring the variation of conductivity through

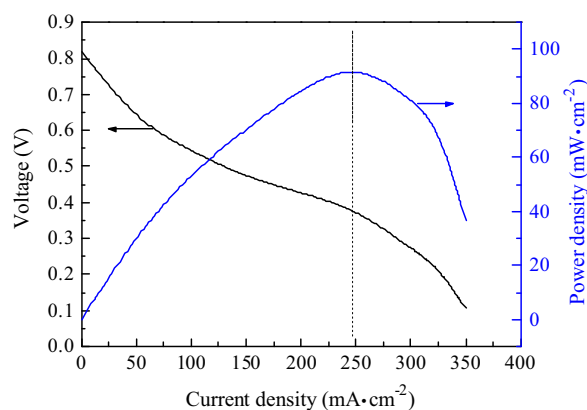


Fig. 14. Polarization curve of a single cell using MIM-CPES-3/1 with air at ambient pressure (50 °C, 100% RH).

immersing the membrane in a 2 M KOH solution at 60 °C. As shown in Fig. 13, the conductivity of the MIM-CPES-3/1 membrane declined sharply in the initial 100 h due to the degradation of imidazolium groups by the attack of OH<sup>-</sup>. Furthermore, the decrease in conductivity is also partly related to the degradation of the crosslinkage in a hot alkaline solution leading to the loss of the quaternary ammonium groups via Hofmann elimination. Some researchers have proposed the degradation mechanism of imidazolium groups based on the results from the <sup>1</sup>H NMR spectra and computational analysis [30–32]. Those investigations suggest that the primary degradation pathway is an imidazolium ring-opening mechanism which is mainly triggered by the nucleophilic attack of OH<sup>-</sup> at the C2 position of the imidazolium ring. After 300 h, the ionic conductivity tended to be constant, and retained around 60% of the original value. And yet for all that, the ionic conductivity is still found to be higher than the magnitude of 10<sup>-2</sup> S cm<sup>-1</sup>. Therefore, the membranes may be suitable for fuel cell applications.

### 3.4. Single cell performance

The MIM-CPES-3/1 membrane was used for the single cell testing given it has the highest ionic conductivity. The single cell equipped with the MIM-CPES-3/1 membrane was evaluated at 50 °C and ambient pressure with fully humidified H<sub>2</sub>/O<sub>2</sub>. Fig. 14 shows the polarization and power density–current density relationship curves. The single cell achieved an open circuit voltage (OCV) of 0.82 V and a maximum power density ( $P_{max}$ ) of 92.1 mW cm<sup>-2</sup> at a current density of 244 mA cm<sup>-2</sup>. The  $P_{max}$  is greater than that of M-5 membrane (30 mW cm<sup>-2</sup>) [31] and 10% crosslinked QPMV-PDVB membrane (80 mW cm<sup>-2</sup>) [33] due to the high conductivity of the MIM-CPES-3/1 membrane. The single cell performance not only lies on the membrane itself, but also associates with the fabrication of the single cell and the operating conditions [34–36]. Therefore, further work will focus on the optimization of the MEA construction, the structure of the single cell and the operational conditions.

## 4. Conclusions

In this work, a series of novel imidazolium crosslinked membranes were fabricated by crosslinking the tertiary amine containing PES (PES-DA) with the bromomethyl containing PES (BPES) via quaternization. The formed crosslinkage not only makes the AEMs have a network structure with an improved dimensional stability,

but also acts as a hydroxyl conductor. In addition, both the polymers contain cardo-type molecules, phenolphthalein or fluorine groups. These larger groups could force each polymer chain apart resulting in large interchain separations (free volume) in which water molecules could be confined. The as-fabricated AEMs exhibit a high hydroxide conductivity, and the swelling at elevated temperature can be effectively suppressed thanks to the cross-linking. A good performance is found for the single cell with the MIM-CPES-3/1. Furthermore, the membranes also show good thermal, alkaline stability and mechanical properties. All the results suggest that the as-prepared membranes are promising for application in alkaline fuel cells.

## Acknowledgments

Financial support from the National Natural Science Foundation of China (Grant no. 21376194), the Nature Science Foundation of Fujian Province of China (Grant no. 2014H0043), and the research fund for the Priority Areas of Development in Doctoral Program of Higher Education (No. 20130121130006) is gratefully acknowledged.

## Nomenclature

$A$	cross sectional area of the tested membrane, $\text{cm}^2$
$IEC$	ionic exchange capacity, $\text{meq g}^{-1}$
$k$	elasticity coefficient of the quartz spring, $\text{N cm}^{-1}$
$l$	distance between the two electrodes, $\text{cm}$
$L_d$	length of the dried membrane, $\text{cm}$
$L_w$	length of the wet membrane, $\text{cm}$
$L_1$	length of the quartz spring, $\text{cm}$
$L_2$	length of the quartz spring loaded with the dried membrane, $\text{cm}$
$L_3$	length of the quartz spring loaded with the swollen membrane, $\text{cm}$
$m_d$	mass of the dried membrane, $\text{g}$
$M_{o, HCl}$	milliequivalent of HCl required before equilibrium, $\text{mmol}$
$M_{e, HCl}$	milliequivalent of HCl required after equilibrium, $\text{mmol}$
$R$	membrane resistance, $\Omega$
$SR$	swelling ratio, %
$W_d$	width of the dried membrane, $\text{cm}$
$W_w$	width of the wet membrane, $\text{cm}$
$WU$	water uptake, %

## Greek letter

$\sigma$	ionic conductivity, $\text{S cm}^{-1}$
----------	--

## References

- [1] M.Z. Jacobson, W.G. Colella, D.M. Golden, Cleaning the air and improving health with hydrogen fuel-cell vehicles, *Science* 308 (2005) 1901–1905.
- [2] M.A. Hickner, H. Ghassemi, Y.S. Kim, B.R. Einsla, J.E. McGrath, Alternative polymer systems for proton exchange membranes (PEMs), *Chem. Rev.* 104 (2004) 4587–4612.
- [3] R. Bashyam, P. Zelenay, A class of non-precious metal composite catalysts for fuel cells, *Nature* 443 (2006) 63–66.
- [4] M. Tanaka, K. Fukasawa, E. Nishino, S. Yamaguchi, K. Yamada, H. Tanaka, B. Bae, K. Miyatake, M. Watanabe, Anion conductive block poly (arylene ether)s: synthesis, properties, and application in alkaline fuel cells, *J. Am. Chem. Soc.* 133 (2011) 10646–10654.
- [5] A. Jasti, V.K. Shahi, Multi-block poly (arylene ether)s containing pre-chloromethylated bisphenol: anion conductive ionomers, *J. Mater. Chem. A* 1 (2013) 6134–6137.
- [6] J.R. Varcoe, R.C. Slade, Prospects for alkaline anion-exchange membranes in low temperature fuel cells, *Fuel cells* 5 (2005) 187–200.
- [7] S.S. He, C.W. Frank, Facilitating hydroxide transport in anion exchange membranes via hydrophilic grafts, *J. Mater. Chem. A* 2 (2014) 16489–16497.
- [8] X. Wu, W. Chen, X. Yan, G. He, J. Wang, Y. Zhang, X. Zhu, Enhancement of hydroxide conductivity by the di-quaternization strategy for poly (ether ether ketone) based anion exchange membranes, *J. Mater. Chem. A* 2 (2014) 12222–12231.
- [9] J. Pan, C. Chen, L. Zhuang, J. Lu, Designing advanced alkaline polymer electrolytes for fuel cell applications, *Acc. Chem. Res.* 45 (2011) 473–481.
- [10] W. Wang, S. Wang, W. Li, X. Xie, Y. Lv, Synthesis and characterization of a fluorinated cross-linked anion exchange membrane, *Int. J. Hydrog. Energy* 38 (2013) 11045–11052.
- [11] N.J. Robertson, H.A. Kostalik IV, T.J. Clark, P.F. Mutolo, H.D. Abruna, G.W. Coates, Tunable high performance cross-linked alkaline anion exchange membranes for fuel cell applications, *J. Am. Chem. Soc.* 132 (2010) 3400–3404.
- [12] T.J. Clark, N.J. Robertson, H.A. Kostalik IV, E.B. Lobkovsky, P.F. Mutolo, H.D. Abruna, G.W. Coates, A ring-opening metathesis polymerization route to alkaline anion exchange membranes: development of hydroxide-conducting thin films from an ammonium-functionalized monomer, *J. Am. Chem. Soc.* 131 (2009) 12888–12889.
- [13] G. Merle, S.S. Hosseiny, M. Wessling, K. Nijmeijer, New cross-linked PVA based polymer electrolyte membranes for alkaline fuel cells, *J. Membr. Sci.* 409 (2012) 191–199.
- [14] J. Zhou, M. Ünlü, I. Anestis-Richard, P.A. Kohl, Epoxy-based anion conductive membranes for alkaline membrane fuel cells, *J. Membr. Sci.* 350 (2010) 286–292.
- [15] H. Sun, G. Zhang, Z. Liu, N. Zhang, L. Zhang, W. Ma, C. Zhao, Q. Duo, G. Li, H. Na, Self-crosslinked alkaline electrolyte membranes based on quaternary ammonium poly (ether sulfone) for high-performance alkaline fuel cells, *Int. J. Hydrog. Energy* 37 (2012) 9873–9881.
- [16] S. Gu, R. Cai, Y. Yan, Self-crosslinking for dimensionally stable, solvent-resistant quaternary phosphonium based hydroxide exchange membranes, *Chem. Commun.* 47 (2011) 2856–2858.
- [17] W. Lu, Z.G. Shao, G. Zhang, Y. Zhao, B. Yi, Crosslinked poly (vinylbenzyl chloride) with a macromolecular crosslinker for anion exchange membrane fuel cells, *J. Power Sources* 248 (2014) 905–914.
- [18] A.H. Rao, S. Nam, T.H. Kim, Crosslinked poly (arylene ether sulfone) block copolymers containing pendant imidazolium groups as both crosslinkage sites and hydroxide conductors for highly selective and stable membranes, *Int. J. Hydrog. Energy* 39 (2014) 5919–5930.
- [19] P.Y. Xu, K. Zhou, G.L. Han, Q.G. Zhang, A.M. Zhu, Q.L. Liu, Fluorene-containing poly (arylene ether sulfone)s as anion exchange membranes for alkaline fuel cells, *J. Membr. Sci.* 457 (2014) 29–38.
- [20] P.Y. Xu, K. Zhou, G.L. Han, Q.G. Zhang, A.M. Zhu, Q.L. Liu, Effect of fluorene groups on the properties of multiblock poly (arylene ether sulfone)s-based anion-exchange membranes, *ACS Appl. Mater. Interfaces* 6 (2014) 6776–6785.
- [21] K. Miyatake, B. Bae, M. Watanabe, Fluorene-containing cardo polymers as ion conductive membranes for fuel cells, *Polym. Chem.* 2 (2011) 1919–1929.
- [22] J. Zheng, J. Wang, S. Zhang, T. Yuan, H. Yang, Synthesis of novel cardo poly (arylene ether sulfone)s with bulky and rigid side chains for direct methanol fuel cells, *J. Power Sources* 245 (2014) 1005–1013.
- [23] Q. Zhang, Q. Zhang, S. Zhang, S. Li, Synthesis and characterization of sulfonated poly (aryl ether sulfone) containing pendent quaternary ammonium groups for proton exchange membranes, *J. Membr. Sci.* 354 (2010) 23–31.
- [24] S. Singh, A. Jasti, M. Kumar, V.K. Shahi, A green method for the preparation of highly stable organic-inorganic hybrid anion-exchange membranes in aqueous media for electrochemical processes, *Polym. Chem.* 1 (2010) 1302–1312.
- [25] B. Lin, L. Qiu, B. Qiu, Y. Peng, F. Yan, A soluble and conductive polyfluorene ionomer with pendant imidazolium groups for alkaline fuel cell applications, *Macromolecules* 44 (2011) 9642–9649.
- [26] Z. Liu, X. Li, K. Shen, P. Feng, Y. Zhang, X. Xu, W. Hu, Z. Jiang, B. Liu, M.D. Guiver, Naphthalene-based poly (arylene ether ketone) anion exchange membranes, *J. Mater. Chem. A* 1 (2013) 6481–6488.
- [27] T.A. Sherazi, J. Yong Sohn, Y. Moo Lee, M.D. Guiver, Polyethylene-based radiation grafted anion-exchange membranes for alkaline fuel cells, *J. Membr. Sci.* 441 (2013) 148–157.
- [28] L. Ye, L. Zhai, J. Fang, J. Liu, C. Li, R. Guan, Synthesis and characterization of novel cross-linked quaternized poly (vinyl alcohol) membranes based on morpholine for anion exchange membranes, *Solid State Ion.* 240 (2013) 1–9.
- [29] G. Nie, X. Li, J. Tao, W. Wu, S. Liao, Alkali resistant cross-linked poly (arylene ether sulfone)s membranes containing aromatic side-chain quaternary ammonium groups, *J. Membr. Sci.* 474 (2015) 187–195.
- [30] B. Lin, H. Dong, Y. Li, Z. Si, F. Gu, F. Yan, Alkaline stable C2-substituted imidazolium-based anion-exchange membranes, *Chem. Mater.* 25 (2013) 1858–1867.
- [31] J. Ran, L. Wu, J.R. Varcoe, A.L. Ong, S.D. Poynton, T. Xu, Development of imidazolium-type alkaline anion exchange membranes for fuel cell application, *J. Membr. Sci.* 415 (2012) 242–249.
- [32] Y. Ye, Y.A. Elabd, Relative chemical stability of imidazolium-based alkaline anion exchange polymerized ionic liquids, *Macromolecules* 44 (2011) 8494–8503.

- [33] Y. Luo, J. Guo, C. Wang, D. Chu, Fuel cell durability enhancement by cross-linking alkaline anion exchange membrane electrolyte, *Electrochem. Commun.* 16 (2012) 65–68.
- [34] Z. Zhang, L. Wu, J. Varcoe, C. Li, A.L. Ong, S. Poynton, T. Xu, Aromatic polyelectrolytes via polyacylation of pre-quaternized monomers for alkaline fuel cells, *J. Mater. Chem. A* 1 (2013) 2595–2601.
- [35] M. Carmo, G. Doubek, R.C. Sekol, M. Linardi, A.D. Taylor, Development and electrochemical studies of membrane electrode assemblies for polymer electrolyte alkaline fuel cells using FAA membrane and ionomer, *J. Power Sources* 230 (2013) 169–175.
- [36] S.D. Poynton, R.C. Slade, T.J. Omasta, W.E. Mustain, R. Escudero-Cid, P. Ocón, J. R. Varcoe, Preparation of radiation-grafted powders for use as anion exchange ionomers in alkaline polymer electrolyte fuel cells, *J. Mater. Chem. A* 2 (2014) 5124–5130.